

# Superfluid $^3\text{He}$ A-B Surface Tension

M. Bartkowiak, R.P. Haley <sup>1</sup>, S.N. Fisher, A.M. Guénault, G.R. Pickett and P. Skyba <sup>b</sup>

*Department of Physics, Lancaster University, Lancaster, LA1 4YB, United Kingdom*

<sup>b</sup>*Institute of Experimental Physics, Slovak Academy of Sciences, Watsonova 43, 04353 Košice, Slovakia*

---

## Abstract

We have made two different measurements of interfacial energies below 300  $\mu\text{K}$ , at zero pressure and in magnetic fields up to 400 mT. A variable magnetic field profile allows us to stabilize and precisely manipulate the position of the A-B interface. First, we can derive the difference in wall wetting energies from the behaviour of the phase boundary as it enters and exits a stack of glass capillary tubes. Secondly, we can measure the surface tension from the level of over- or under-magnetization needed to force the interface through an aperture. These are the first surface energy measurements in high magnetic fields in the zero-temperature limit. Our results are in surprising agreement with earlier measurements at high pressure close to  $T_c$ .

*Key words:* superfluidity; helium-3; interface; wetting

---

## 1. Introduction

The phase interface between the A and B phases of superfluid  $^3\text{He}$  is unique in providing the highest symmetry interface available for experimental study[1]. The system is inherently free of any defects and impurities. The two bulk coherent ‘parent’ phases are well understood. However, the complexity of the superfluid  $^3\text{He}$  order parameter means that the evolution across the interface is very complex. This boundary certainly provides a structure well worth further investigation. A fundamental property of such a first-order transition is the finite “stiffness” of the boundary and the associated energy or surface tension. Since we in principle know the structure of the parent phases a good experimental value for the surface tension is a valuable input quantity for both experimental and theoretical understanding of this interface. The surface tension is also an important parameter in understanding the phase-nucleation mechanisms in superfluid  $^3\text{He}$ , which remain a hotly-debated subject[1].

In this paper we present measurements of the AB surface tension at 0 bar and  $\sim 0.2T_c$ . This energy has already been measured for temperatures down to  $0.5T_c$  at melting pressure [2], where extensive calculations are available. However, the only available theoretical prediction at low pressure [3] is valid towards the Ginzburg-Landau region where the AB phase transition is predicted to be continuous and the surface tension vanishes.

## 2. Experiment

Two experiments have been made in the inner cell of a Lancaster-style nested nuclear demagnetisation stage [4]. The outer cell, containing copper powder and  $^3\text{He}$  at around 1 mK, acts as a thermal guard. The  $^3\text{He}$  in the inner cell is cooled by silver-sintered copper plate refrigerant. The inner cell fluid is connected through a small orifice to an experimental tailpiece which constitutes a quasiparticle blackbody radiator(BBR) [4,5], as shown in figures 1 and 2. At zero bar and with the bottom of the cell in a field of 400 mT, the  $^3\text{He}$  in the tailpiece can be cooled below 200  $\mu\text{K}$ .

---

<sup>1</sup> email: r.haley@lancaster.ac.uk

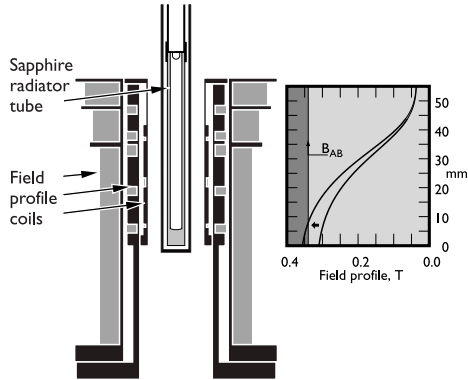


Fig. 1. Sapphire tube black body radiator surrounded by solenoid assembly, shown with a typical magnetic field profile.

The radiator volume contains heater and thermometer vibrating wire resonators (VWR). The frequency width or damping of the resonance,  $\Delta f_2$ , is proportional to quasiparticle density, and varies as  $\exp(-\Delta_B/k_B T)$  in the B phase, where  $\Delta_B$  is the B phase energy gap. Power enters the radiator by residual heat leaks and from motion of the AB interface, and is calibrated using the VWR heater. In equilibrium the excitation flux leaving the orifice carries away all the incoming power. The equilibration time is on the order of 10 s, governed by the thermal impedance of the orifice and the heat capacity inside the BBR.

A set of superconducting solenoids, thermally anchored to the still of the dilution refrigerator, provide the magnetic field profiles we use to create, stabilise and manipulate the AB interface inside the tailpiece (Fig. 1). The largest solenoid provides the bulk of the 340 mT critical field,  $B_{AB}$ , required to nucleate A phase from B phase [6–8], but with the profile shaped to ensure that the field is always below 50 mT at the VWR's. A smaller solenoid is used to make the profile more linear in the region of interest, and a set of opposing Helmholtz pair coils are used to control the gradient.

When the interface moves inside the BBR, latent heat  $L$  is released or absorbed as A phase converts to B phase or vice versa. This is measured by the VWR as a deviation in damping from the background level. For a cylindrical volume of cross-sectional area  $S$ , when the AB interface is moved along its axis at velocity  $v$  by ramping the solenoid currents, the heat released is  $-LSv$ . Under quasi-equilibrium conditions the AB boundary sits at the position of the bulk critical field. As the field ramps at rate  $\dot{B}$ , the interface velocity is  $v = \dot{B}/\nabla B$  where  $\nabla B$  is the local field gradient. The principle of the two experiments described here is to move the interface through BBR's containing capillaries or small holes, and observe transient heating/cooling features when the interface position be-

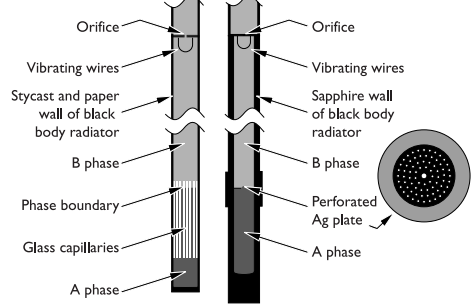


Fig. 2. Left: capillary cell. Right: grid cell.

comes de-coupled from the bulk critical field owing to capillary action or trapping at a grid by surface tension.

We first measured the wall energy difference between the A and B phase wetting silica glass. The methods used have been previously reported [9], though this paper contains a refined result following further measurements. The radiator contained a stack of 58 glass capillaries with inner diameter 0.45 mm separating the upper and lower bulk volumes. We first defined a particular field profile using the whole solenoid set, and then ramped the current in the largest solenoid to move the phase boundary through the capillary stack along this profile. Starting with A phase in the bottom, and the interface below the stack, we monitored the change in VWR damping as the AB boundary moved up through the capillaries. We observed that capillary action pulls the boundary up inside the tubes since A phase wets preferentially over B phase. From features on the VWR trace we measured the difference between bulk critical field and field at the interface position. We then used the known magnetisation difference at the AB transition [7] to calculate the difference in wall energy.

In the capillary experiment we also observed the trapping of the interface at the tube ends by surface tension, followed by escape as the bulk equilibrium position moves up away from the stack. However, for reasons discussed below these events could not be measured with sufficient reliability. This led to the second set of ongoing experiments in which we measure the interface “popping” through a well-defined hole geometry.

In using the BBR method there is a trade-off between time constants and ramp rates. The interface must be ramped fast enough that the cooling/warming can be seen over the background level. However, owing to the BBR time constant of 10–15 seconds, it must also move slowly enough that cooling/warming transients associated with the pinning and popping at apertures can be resolved. A major consideration is aperture size: too large and the interface will not be held back long enough to allow us to observe any transients; too small and the interface will be held so strongly that we can-

not unpin it with the fields available to us. Since we already observed the interface breaking free of the capillary tube ends, we knew that a hole of approximately 0.4 mm diameter was optimum.

A further consideration is that we must be able to suppress nucleation events from occurring before the interface pops though the hole. Previous nucleation measurements [6] have shown that sapphire-walled cells are sufficient for this purpose. Sapphire also has the advantage over Styccast or Kapton that background heating effects associated with changing magnetic fields are almost negligible.

Our first preference was to make the apertures in glass for ease of comparison with the capillary experiment. However, we found it exceedingly difficult and expensive to produce a thin flat plate of glass containing a large number of quality sub-millimetre holes. We decided to make our own grid of holes in a 0.12 mm thick plate of silver. Part of the uncertainty in the capillary cell measurements was due to radial field gradients and variable roughness in the cut tube ends. We drilled a single well-defined 0.4 mm hole in the centre of the plate, and surrounded it by 74 0.2 mm holes. Thus we could be sure that the interface would escape first from the central large hole where radial field gradients are unimportant. The smaller holes provide ample thermal contact through the BBR. To reduce potential nucleation sites, the silver was buffed and polished to supposed optical quality with 0.3  $\mu\text{m}$  alumina powder. It was then carefully cleaned to remove all traces of the powder, and examined using large-area-scan AFM. These images showed scratches and pits on the 0.1-1  $\mu\text{m}$  scale. However, we never observed any of the history-dependence or stochasticity which would be associated with nucleation [6].

The perforated silver plate was finally sandwiched between two halves of a sapphire tube (inner diameter 4.25 mm, length 47 mm) and glued with Styccast 2651. For optimum control over the field profile at the apertures, we tried to position the grid at the centre of the gradient coils. However, from measurements of the motion of the boundary through the cell we ascertained that the grid was between 2.0 and 2.5 mm below the gradient coil centre, presumably owing to differential thermal contraction during cool-down. The measurements are so sensitive to the boundary motion that we can even resolve the 0.12 mm thickness of the silver grid in the features that we observe.

### 3. Results and Discussion

Figure 3 shows ramps for the interface moving through the grid cell, and in the capillary cell for comparison. In both ramp directions the A phase is at the

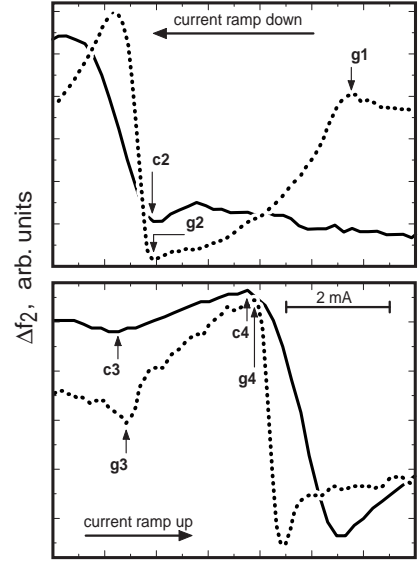


Fig. 3. Current ramps for the grid (dotted line) and capillary (solid line) cells with the associated change in vibrating wire damping,  $\Delta f_2$ . Labelled features are explained in the text.

bottom of the cell separated from the B phase above by the interface. In the down ramp, current to the main solenoid is decreased and the boundary moves down the cell, converting A to B and giving rise to a warming effect above the background.

At g1 the interface reaches the grid and is held there by surface tension. The ramp continues, but with a stationary interface no heat is released, and the VWR damping relaxes back to the background level. The bulk equilibrium position of the AB boundary moves below the grid, and the interface is left behind in a region of increasing under-magnetisation.

At g2 enough free energy is available for the interface to unpin from the central hole of the grid and it pops off. The B phase fills the volume down to the bulk equilibrium position and gives a sharp transient warming.

In the up ramp there is a cooling effect as B converts to A and absorbs latent heat. The interface is trapped on the grid at g3 and pops off at g4. One can immediately see that it is easier to identify the more pronounced features g1-4 in the grid cell than it is to judge the corresponding positions of features c2-4 in the capillary cell. In the capillary cell we also had to combine features on up and down ramps making us vulnerable to hysteretic effects in the superconducting solenoids. With the grid cell we are able to determine the surface energy to better than 10%, compared with around 25% for the capillaries.

In zero field gradient, under-magnetised B phase will pop off the aperture when the bubble becomes hemispherical (in higher gradients, minimizing the surface vs. volume free energy leads to shapes which are

squashed in the field gradient direction). This occurs when the volume free energy,  $\Delta G$ , exceeds  $2\sigma_{AB}/r_h$  where  $\sigma_{AB}$  is the AB surface energy and  $r_h$  is the hole radius. At the hole  $\Delta G$  is given by  $\frac{1}{2}\Delta\chi(B_{AB}^2 - B_h^2)$  where  $B_h$  is the field at the hole, and  $\Delta\chi$  is the magnetic susceptibility difference between A phase and *magnetised* B phase. The interface then pops off the aperture when

$$B_{AB} - B_h = \frac{2\sigma_{AB}}{\Delta M_{AB}r_h},$$

where we have assumed  $B_{AB} - B_h \ll B_{AB}$ , and in order to account for B phase distortion we have replaced  $\Delta\chi B_{AB}$  by the measured magnetisation difference  $\Delta M$  [7]. We deduce the field difference  $B_{AB} - B_h$  from the measured currents at features g1 and g2, and the known field profile.

Combining many measurements of  $\sigma_{AB}$  from down ramps using various field profiles then gives a consistent value of  $\sigma_{AB} = (3.58 \pm 0.24) \times 10^{-9} \text{ Jm}^{-2}$ . This is lower but in agreement with  $(4.6 \pm 1.3) \times 10^{-9} \text{ Jm}^{-2}$  as estimated from the capillary experiment [9]. That experiment gave a more reliable value for the difference in wall energy between the A and B phases wetting silica glass,  $\sigma_{BW} - \sigma_{AW} = (1.36 \pm 0.11) \times 10^{-9} \text{ Jm}^{-2}$ . The two measurements may be combined to give the contact angle  $\theta$  using the relation  $\sigma_{BW} - \sigma_{AW} = \sigma_{AB} \cos\theta$ . This gives a contact angle of  $68^\circ \pm 4^\circ$  on silica glass, in remarkably good agreement with the value of  $68^\circ$  obtained by Osheroff [10] on glass at melting pressure.

There is an added complication for the up ramp where we pull A out into B phase. The current difference between features such as g3-g4 is always less than g1-g2. Assuming that the A phase preferentially wets the silver, the interface reaches the contact angle with the grid surface before it becomes hemispherical. At this point the interface can grow out across the grid surface to fill the available volume. This occurs at a lower free energy difference than that for the B phase popping.

In principle one could combine the B and A phase measurements to calculate a contact angle on the silver grid. However this would require the hole edges to be smooth on the scale of the interface thickness (a few coherence lengths). As mentioned above the surface is in fact quite rough on this scale, which allows the A phase to escape earlier than expected. This is consistent with our observations.

In the absence of any theoretical calculations of the surface tension outside the Ginzburg-Landau regime, all we can do is to compare our measured values with those of Osheroff by using the expected relation  $\sigma_{AB} \sim F_0 \xi (f/F_0)^{1/2}$ . Here  $\xi$  is the temperature-dependent coherence length,  $F_0$  the difference between the normal phase and superfluid free energies at  $T_{AB}$ , and  $f$  the maximum additional free energy

associated with the order parameter distortion within the interface. Scaling down from melting pressure to our pressure and temperature regime would give  $\sigma_{AB} = 5.6 \times 10^{-9} \text{ Jm}^{-2}$  at  $200 \mu\text{K}$  if  $(f/F_0)^{1/2}$  remains constant. This is in good agreement with our measured value above, given that we have no choice but to extrapolate from a completely different part of the phase diagram. However, Thuneberg has calculated that in the Ginzburg-Landau regime  $(f/F_0)^{1/2}$  may decrease by a factor of up to 2.5 between melting and zero pressure [3].

Therefore we can say in conclusion that these first measurements of the AB surface tension in the zero-temperature limit are in surprisingly good agreement with previous measurements on the assumption that  $(f/F_0)^{1/2}$  is only slowly varying. Since we have no real reason to assume this, there is clearly a need for calculations to be made in the high-field low temperature regime.

## Acknowledgements

We thank M. Ward and I. Miller for their excellent technical support, R. Blaauwgeers for many useful discussions, and the UK EPSRC for financial support.

## References

- [1] A.J. Leggett, S.K. Yip, *Helium Three*, edited by W.P. Halperin and L.P. Pitaevski (Elsevier, 1990), p.523.
- [2] D.D. Osheroff, M.C. Cross, *Phys. Rev. Lett.* **38**, 905 (1977).
- [3] E.V. Thuneberg, *Phys. Rev. B* **44**, 9685 (1991).
- [4] S.N. Fisher, A.M. Guénault, C.J. Kennedy, G.R. Pickett, *Phys. Rev. Lett.* **69**, 1073 (1992), with temperature scale modification of C. Bäuerle, Yu.M. Bunkov, S.N. Fisher, H. Godfrin *Phys. Rev. B* **57**, 14381 (1998).
- [5] M. Enrico, S.N. Fisher, A.M. Guénault, G.R. Pickett, K. Torizuka *Phys. Rev. Lett.* **70**, 1846 (1993).
- [6] M. Bartkowiak, S.N. Fisher, A.M. Guénault, R.P. Haley, G.R. Pickett, G.N. Plenderleith, P. Skyba *Phys. Rev. Lett.* **85**, 4321 (2000).
- [7] M. Bartkowiak, S.W.J. Daley, S.N. Fisher, A.M. Guénault, R.P. Haley, G.R. Pickett, G.N. Plenderleith, P. Skyba *Phys. Rev. Lett.* **83**, 3462 (1999).
- [8] I. Hahn, Y.H. Tang, H.M. Bozler, C.M. Gould, *Physica* (Amsterdam) **194-196B**, 815 (1994).
- [9] M. Bartkowiak, S.N. Fisher, A.M. Guénault, R.P. Haley, G.R. Pickett, M.C. Rogge, P. Skyba, *J. Low Temp. Phys.* **126**, 533 (2002).
- [10] J. Landau, A.E. White, D.D. Osheroff (*unpublished*) and private communication with D.D. Osheroff.